

# Rational design of visible and NIR distyryl-BODIPY dyes from a novel fluorinated platform†

Olivier Galangau, Cécile Dumas-Verdes, Rachel Méallet-Renault and Gilles Clavier\*

Received 31st March 2010, Accepted 30th June 2010

DOI: 10.1039/c004812g

A new series of distyryl-BODIPY has been rationally designed and synthesised from a novel fluorinated platform, 8-pentafluorophenylBODIPY, which has enhanced reactivity in the presence of both electron rich, and for the first time, electron deficient aldehydes. The pentafluorobenzene leads to larger red shifts of absorption and emission compared to previously reported analogues. The reactivity and spectroscopic results have been rationalised with quantum mechanics calculation. The fluorescence sensitivity of one derivative to acidity is also presented.

## Introduction

Near-infrared fluorophores are the object of intense research because of their potential applications in many domains. Indeed, this range of the electromagnetic spectrum is seldom used because of the lack of suitable chromophores while applications such as photodynamic therapy or non-invasive imaging probes would benefit greatly from such molecules.<sup>1</sup> Photovoltaism also needs molecules capable of absorbing this tail of the solar spectrum<sup>2</sup> and OLED<sup>3</sup> research is in need of pure red emitting fluorophores. 4,4-Difluoro-4-bora-3a,4a-diaza-*s*-indacene, commonly known as the trademarked name BODIPY, has been recognised as a very convenient fluorophore in many areas. Among them, BODIPYs are commercially available as biological labels and laser dyes.<sup>4</sup> But many derivatives have been developed for other applications such as light harvesting,<sup>5</sup> fluoroionophores,<sup>6</sup> fluorescent switches,<sup>7</sup> photosensitisers<sup>8</sup> and energy transfer cassettes.<sup>9</sup> This interest in the BODIPY core stems from its outstanding photophysical properties, namely high absorption coefficient and fluorescence quantum yield, good photostability, and little sensitivity to the medium (weak solvatochromism and halochromism).<sup>10</sup> In addition, its synthesis allows for relatively easy modification of the substituents around the diazaindacene core. Indeed, this can be done by varying the nature of the starting pyrroles (providing they're available) or carbonyl derivative (aldehyde or acid chloride), as well as by post-functionalization in various positions. Depending on their location on the BODIPY core, these substituents can have a strong influence on the position of the absorption and emission maxima which can shift from *ca.* 500 nm for a simple derivative to 620 nm for compounds substituted by large aromatics (Fig. 1). Very important shifts toward the NIR end of the visible spectra have been recently achieved by two approaches. One is the replacement of the *meso* carbon (*i.e.* in position 8) by a nitrogen atom yielding the so called aza-BODIPY.<sup>11</sup> Several research groups have also developed a synthetic approach which is based on a Knoevenagel type condensation between selected aldehydes and a BODIPY

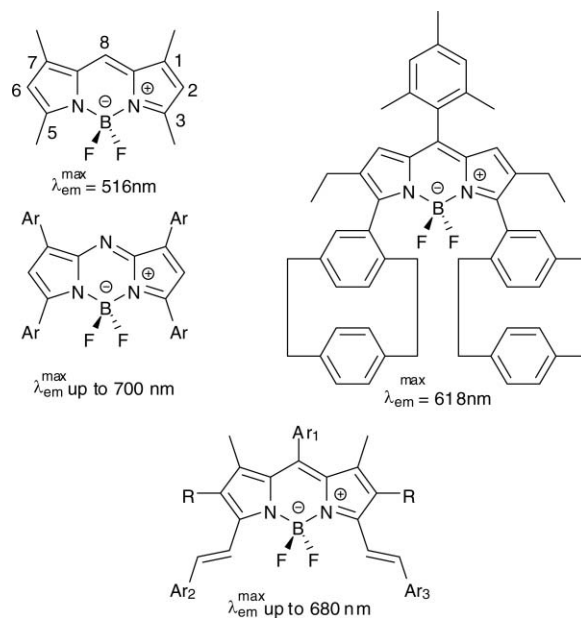


**Fig. 1** Representative BODIPY derivatives and their maximum emission wavelength (numbers on the left structure refers to the common numbering of the diaza-*s*-indacene moiety).

comprising two methyl groups in the 3 and 5 positions.<sup>12</sup> The reaction affords, depending on the conditions, the mono or distyryl substituted derivatives.

As part of our research on BODIPY derivatives for solid state fluorescence,<sup>13</sup> we decided to investigate this reaction for our needs. We also reasoned that enhancing the donor acceptor balance between the styryl and BODIPY part would further shift its fluorescence toward the red. For this purpose, a careful examination of the electron density change upon excitation of the BODIPY revealed that in the excited state, the carbon in position 8 experiences a marked increase in electron density. We then surmised that introducing a strong electron acceptor such as pentafluorobenzene on that position would increase the emission's bathochromic shift compared to similar reported distyryl BODIPY. Preliminary calculations also demonstrated an increase in the partial charge of the 3 and 5 methyl protons when going from phenyl to pentafluorophenyl which should result in a

PPSM, ENS Cachan, CNRS, UniverSud, 61 av President Wilson, F-94230, CACHAN, France. E-mail: gilles.clavier@ppsm.ens-cachan.fr; Fax: 33 1 47 40 24 54; Tel: 33 1 47 40 27 02

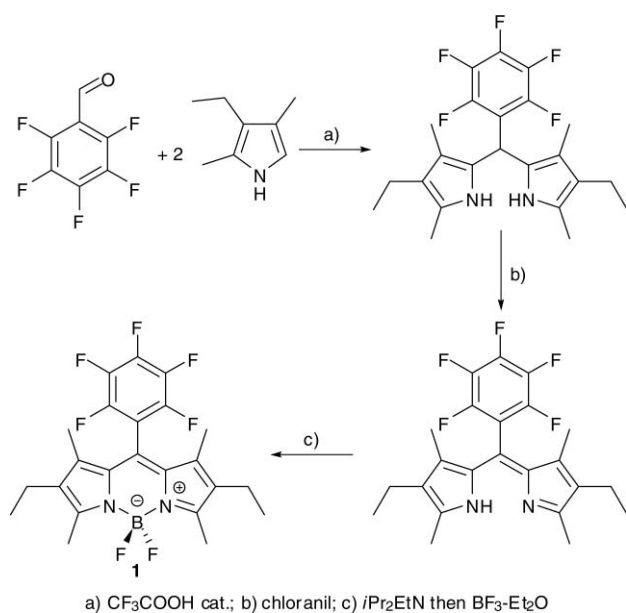
† Electronic supplementary information (ESI) available: NMR spectra, spectroscopic results and molecular modelling. See DOI: 10.1039/c004812g

higher reactivity. Herein, we will present the optimised synthesis of BODIPY **1**, its subsequent derivatisation with styryl using aldehydes of different nature and the photophysical properties in solution of the obtained red emissive fluorophores.

## Results and discussion

### Synthesis

The starting pentafluorophenyl BODIPY was synthesised according to the three step one-pot classical approach starting from pentafluorobenzaldehyde and two equivalents of 3-ethyl-2,4-dimethylpyrrole in the presence of a catalytic amount of trifluoroacetic acid followed by oxidation and complexation with boron difluoride (Scheme 1). The oxidation step was first done using dichlorodicyano-benzoquinone (DDQ). But this oxidant revealed to be problematic because a lot of a side BODIPY product with a hydrogen atom in the 8 position was obtained. It was concluded that this oxidant causes extensive cleavage of the carbon-carbon bond and was replaced by the less reactive chloranil. The exposition time was also optimised and the reaction was shortened to a few minutes. BODIPY **1** was thus obtained in 90% overall yield.



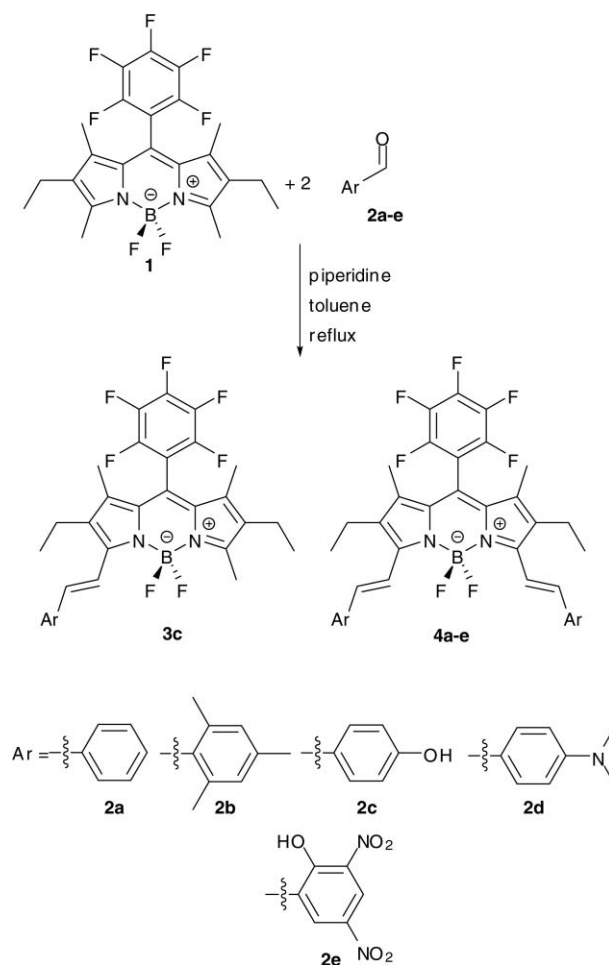
**Scheme 1** Synthesis of the pentafluorophenyl substituted BODIPY **1**.

The introduction of two styryl groups was then attempted with benzaldehyde and other aryl aldehydes with electron rich substituents following reported procedures using piperidine and acetic acid in refluxing toluene and Dean–Stark apparatus to remove water.<sup>12</sup> Unfortunately, in our hands, this reaction did not give satisfactory results as the expected product was obtained in very low yields together with many other side products which were very difficult to isolate in pure form. The reaction was repeated with success, but after removal of acetic acid from the media and using two equivalents of piperidine. Surprisingly, the only product isolated was the disubstituted one in 13% yield. The monostyryl has been detected as traces on TLC in the form of a blue spot but could not be recovered after chromatography (Table 1 entry 1).

**Table 1** Reaction conditions and yields for the Knoevenagel reaction with BODIPY **1**

Entry	Aldehyde	Reaction time (h)	Eq. piperidine	Yield <b>3a–e</b> (%)	Yield <b>4a–e</b> (%)
1	<b>2a</b>	24	2	not isolated	13
2	<b>2a</b>	48	4	not isolated	not isolated
3	<b>2b</b>	48	3	no reaction	no reaction
4	<b>2b</b>	48	4	not isolated	21
5	<b>2c</b>	48	2	31	37
6	<b>2c</b>	72	4	9	0
7	<b>2d</b>	48	3	0	38
8	<b>2e</b>	48	4	0	36

Longer reaction times and excess base only afforded a complex mixture of products from which the desired compound could not be isolated. The scope of the reaction was then studied using different aromatic aldehydes (Scheme 2 and Table 1).



**Scheme 2** Synthesis of mono- and distyryl-BODIPY derivatives from BODIPY **1**.

The reaction was carried out satisfactorily with the bulky mesitaldehyde, the electron donating *p*-hydroxy- and *p*-dimethylamino-benzaldehyde. More notably, the electron deficient 3,5-dinitrosalicylaldehyde also reacted to give **4e** in reasonable yield (36%). To the best of our knowledge, this is the first time that an electron deficient aldehyde successfully undergoes Knoevenagel reaction with a BODIPY. In any case the major, if not only, product

isolated after column chromatography is the green coloured dialkenyl derivative. The singly substituted blue coloured one was only obtained in sizable amount with hydroxybenzaldehyde (Table 1 entry 5). Reaction times vary from one to two days and it is best to use equimolar amounts of base and aldehyde. In some cases (entries 4, 7 and 8 in Table 1), a side product could be detected. It was isolated after column chromatography in 6.5% yield with aldehyde **2d**.  $^{19}\text{F}$  NMR and mass spectrometry revealed that the product is a BODIPY where a fluorine atom on the *meso* benzene has been substituted by piperidine. This is not surprising if one considers that penta-fluorobenzene can undergo nucleophilic substitution with amines.<sup>14</sup> Despite the potential usefulness of this reaction for the functionalization of BODIPY it was not studied further. In order to avoid obtaining such side product, we repeated the reaction with **2d** (Table 1 entry 7) with non nucleophilic bases. DBU only led to degradation of the starting BODIPY. DABCO led to a slower reaction than piperidine because the mono substituted derivative **3d** was the only isolated compound in poor yield (15%) after 24 h reaction time and no evidence of disubstituted product could be seen on TLC.

### Spectroscopic studies

Absorption and emission spectra of all compounds have been recorded in solution in dichloromethane, except **4e** which is poorly soluble in this solvent and was studied in acetone instead (Fig. 2). They all possess characteristic features of BODIPY: intense visible  $S_1 \leftarrow S_0$  absorption band, narrow emission band and a small

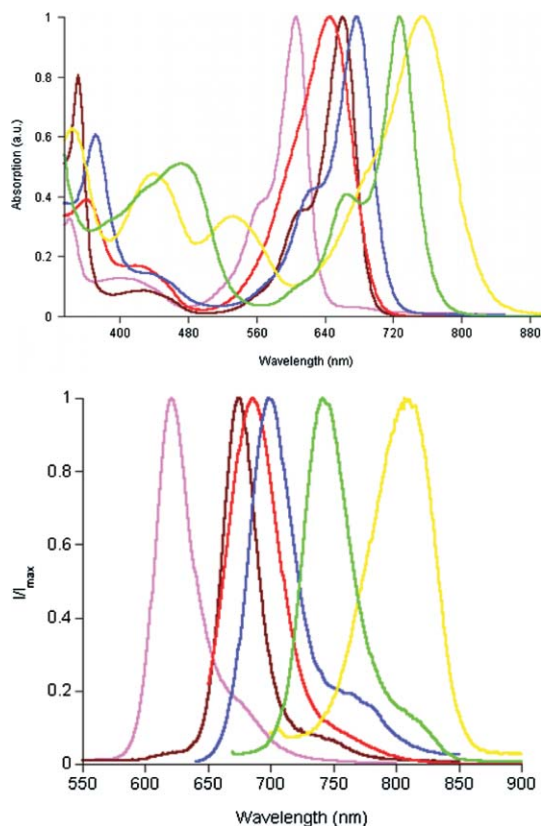


**Fig. 2** Normalised absorption (top) and emission (bottom) spectra of compounds **3c** (pink), **4a** (brown), **4b** (red), **4c** (blue), **4d** (yellow) and **4e** (green).

**Table 2** Photophysical properties in dichloromethane solution

	$\lambda^{\text{abs}}/\text{nm}$	$\epsilon \times 10^{-3}/\text{mol L}^{-1} \text{cm}^{-1}$	$\lambda^{\text{em}}/\text{nm}$	$\phi_{\text{F}}$	$\tau_{\text{F}}^b$	$\Delta\bar{\nu}/\text{cm}^{-1}$	$k_{\text{r}}^c/10^8\text{s}^{-1}$	$k_{\text{nr}}^e/10^8\text{s}^{-1}$
<b>1</b>	544	52	558	0.99	—	461	—	—
<b>3c</b>	606	26	621	0.82	7.7 <sup>f</sup>	399	1.06	0.24
<b>4a</b>	661	80	675	0.59	5.6	314	1.05	0.73
<b>4b</b>	646	55	685	1.00	4.8	881	2.08	0.00
<b>4c</b>	677	81	700	0.66	3.2	506	2.08	1.05
<b>4d</b>	754	62	808	— <sup>d</sup>	—	886	—	—
<b>4d</b> + H <sup>+</sup>	658	—	671	0.34	6.2	294	0.54	1.07
<b>4e</b>	727	64	742	0.15	2.2 <sup>f</sup>	278	0.68	3.87

<sup>a</sup> Excitation was set equal to  $\lambda^{\text{abs}}$ ; <sup>b</sup>  $\lambda_{\text{ex}} = 695 \text{ nm}$ ; <sup>c</sup>  $k_{\text{r}} = \Phi_{\text{F}}/\tau_{\text{F}}$ ;  $k_{\text{nr}} = (1 - \Phi_{\text{F}})/\tau_{\text{F}}$ ; <sup>d</sup> Too small to be measured accurately; <sup>e</sup> Recorded in acetone; <sup>f</sup>  $\lambda_{\text{ex}} = 495 \text{ nm}$ .

Stokes shift ( $\Delta\bar{\nu}$ ). Fluorescence excitation spectra are identical to absorption ones and are mirror image of the fluorescence emission (see ESI†) which indicates that the emitting species are the same as the absorbing ones. First of all, it is interesting to note that the spectroscopic characteristics of BODIPY **1** differ from those of the related derivative bearing a phenyl ring in the 8 position. Indeed both absorption and fluorescence maxima are shifted toward the red by 20 nm and the fluorescence quantum yield is improved as it is close to unity for **1** as compared to  $\approx 0.85$  for the non fluorinated analog.<sup>7a,15</sup> Hence the introduction of an electron withdrawing group on the *meso* position does indeed influence the spectroscopic behaviour of the BODIPY core because of a better stabilisation of the lowest unoccupied molecular orbital (*vide infra*).

Introduction of styryl groups induces a red shift of both absorption (from 60 up to 200 nm) and emission (from 60 up to 250 nm) maxima. The amplitude depends on the aromatic used (Table 2). Hence by simply choosing the proper starting aldehyde one can turn BODIPY **1** into a fluorophore whose emission can be tuned along the visible spectra from 600 to 800 nm highlighting the usefulness of this simple transformation. When compared to non fluorinated analogues, a bathochromic shift in favour of BODIPY **4a–e** is observed.<sup>12,16</sup> This shift ranges from 20 up to 55 nm depending on the nature of the styryl group and is attributed to a better stabilisation of the LUMO in BODIPY **4a–e** by the electron withdrawing pentafluorophenyl moiety. Interestingly, other parameters (absorption coefficient, fluorescence quantum yield and lifetime) are comparable to related dialkenyl BODIPY.

**4b** possess the highest absorption energy in this series and a relatively large Stokes shift ( $880 \text{ cm}^{-1}$ ) when compared to other BODIPY. It has been shown that, a mesityl group directly connected to a BODIPY is orientated perpendicular to the BODIPY plane because of the two *ortho* methyl groups.<sup>13c</sup> In the case of **4b**, it is likely that a similar situation is found in the ground state between the mesityl and the ethenyl as its absorption band is higher in energy than that of **4a**. But a geometrical rearrangement toward a more planar structure must take place in the excited state because its fluorescence emission maximum lies lower in energy than that of **4a**.

The absorption solvatochromism of BODIPY **4a** and **b** have been studied in 6 different solvents (Table 3). In the case of **4a**, only a weak dependence on the solvent has been found ( $254 \text{ cm}^{-1}$ ) as observed for most BODIPY derivatives. On the other hand, **4b** displays a larger shift ( $1541 \text{ cm}^{-1}$ ). No clear fit could be found with usual solvent parameters such as  $E_{\text{T}}(30)$  or electric dipolar moment

**Table 3** Comparison of experimental and calculated results for the absorption maxima

	$\lambda_{\max}^{\text{abs}}/\text{nm}^a$	$\lambda_{\text{calc}}^{\text{abs}}/\text{nm}^b$	R (%) <sup>c</sup>	$f_{\text{calc}}^b$
<b>1</b>	544	450	17.3	0.50
<b>3c</b>	606	536	11.6	0.84
<b>4a</b>	661	577	12.7	0.86
<b>4b</b>	646	623	3.6	0.78
<b>4c</b>	677	599	11.5	0.87
<b>4d<sup>d</sup></b>	754	699 (776)	7.3 (-2.9)	0.79 (0.89)
<b>4d + 2H<sup>+</sup></b>	658	607	7.8	0.87
<b>4e<sup>e</sup></b>	727	616 (642)	15.3 (11.1)	0.47 (0.56)

<sup>a</sup> Experimental value; <sup>b</sup> Calculated value (PBE0/6-311+g(d,p)); <sup>c</sup> Reliability factor;

$$R = \frac{(\lambda_{\max}^{\text{abs}} - \lambda_{\text{calc}}^{\text{abs}})}{\lambda_{\max}^{\text{abs}}} \times 100.$$

<sup>d</sup> Values in parenthesis have been obtained in dichloromethane (IEFPCM method). <sup>e</sup> Values in parenthesis have been obtained in acetone (IEFPCM method)

for either molecule. We thus turned to a generalized treatment of the solvent effect recently proposed by Catalán<sup>17</sup> which is based on four orthogonal empirical scales: the solvent polarizability (*SP*), dipolarity (*SdP*), acidity (*SA*) and basicity (*SB*). The absorption wavenumber ( $\bar{\nu}$ ) is fitted with these solvent parameters according to the equation:

$$\bar{\nu} = \bar{\nu}^{\circ} \mp aSP \mp bSdP \mp cSA \mp dSB$$

where  $\bar{\nu}^{\circ}$  is the gas phase wavenumber, and *a*, *b*, *c* and *d* are the regression coefficients describing the sensitivity of  $\bar{\nu}$  to the different parameters. In both cases we obtained satisfactory results ( $R^2 > 0.96$ ) with this approach (see ESI for details<sup>†</sup>). From this treatment, it can be seen that the *SP* (solvent polarizability) parameter is predominant in both cases. It is not very surprising because, this parameter has been developed to describe the inductive and dispersive components of solute–solvent interactions.<sup>18</sup> In particular, it is well adapted to describe the solvatochromism of nonpolar solute. This fits with the observation that the  $S_1 \leftarrow S_0$  transition of BODIPY **4a** is essentially located on the BODIPY (*vide infra*). The larger shift for BODIPY **4b** is thus attributed to the ability of the solvents to stabilise a planar structure between the BODIPY and the alkenyles.

BODIPY **4d** presents the red most spectra of the series but is only weakly fluorescent. In fact, its fluorescence quantum yield was not determined because of large errors in its measurement. We attribute this weak fluorescence to an efficient quenching of the excited state by electron transfer from the donor nitrogen atoms to the BODIPY acceptor. The presence of the two amine functions prompted the study of its sensitivity to the acidity of the medium. The addition of 2 eq. of trifluoroacetic acid induced a dramatic effect on its photophysical properties (Fig. 3). The absorption and fluorescence spectra are shifted hypsochromically by 96 nm and 137 nm respectively. Furthermore the fluorescence intensity is increased by 45 fold even though it is not fully protonated as seen by comparing the absorption and excitation spectra which are clearly different (Fig. S20<sup>†</sup>). Thus BODIPY **4d** is a good candidate for developing near IR acidity sensors.

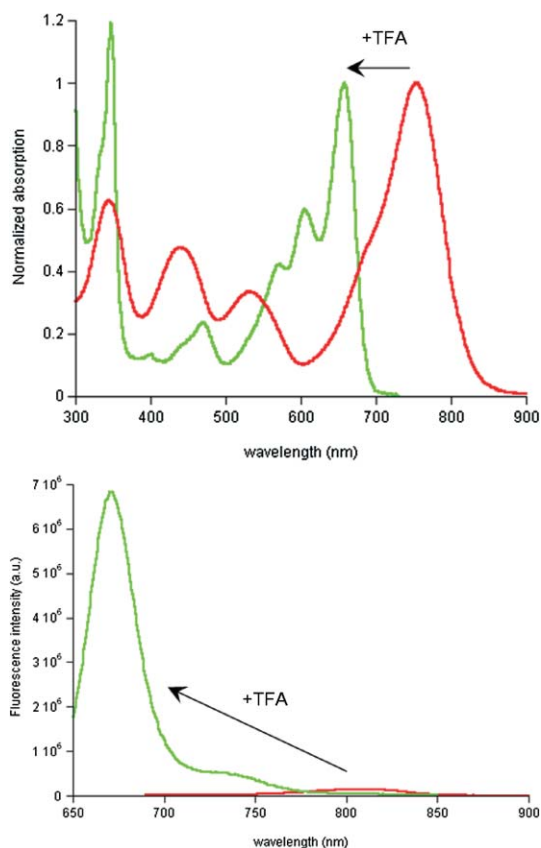


**Fig. 3** Absorption (normalised, top) and fluorescence (bottom) spectra of **4d** (red) and **4d** + 2 eq. of trifluoroacetic acid (green) in dichloromethane (fluorescence spectra were recorded in the same conditions).

### Molecular modelling

Geometry of BODIPY **1** has been optimised by DFT method (B3LYP) using the 6-31g(d) basis set and compared to a non fluorinated model. They have very similar minimised structure to the *meso* phenyl ring orthogonal to the planar BODIPY core and a tetragonal boron (see ESI<sup>†</sup>). The HOMO and LUMO of BODIPY **1** are lower in energy than those of the non fluorinated counterpart by 0.27 and 0.42 eV respectively. This does explain the bathochromic shift observed for BODIPY **1**.

All the geometry of the styryl compounds have been optimised using the same method. In all cases, the BODIPY core was found to be planar and the boron atom to be tetrahedral with the two fluorine atoms perpendicular to the BODIPY plane. As expected from the size of the substituents, the pentafluorophenyl is nearly perpendicular to the BODIPY plane with angles varying from 74 to 89°. The main discrepancies are found on the relative orientation of the styryl substituents *viz.* the BODIPY. Indeed the double bonds are found to be slightly out of plane from the BODIPY by an angle which strongly depends on the appended aromatic unit. They are found to be almost coplanar in the case of BODIPY **4d** (9.6°) while a twist of 28.6° is found in **4e** with intermediate situation for the other derivatives. The twist is then related to electron donating strength of the aromatic. It must be noted that for BODIPY **4b** the calculation tends to a dissymmetrical structure with one styryl at 15.8° which is similar to the phenol and one at 23.6°. This result is surprising and is probably not a good picture

of the actual structure of the molecule. An alternate geometry where the mesityl groups are fixed at a  $90^\circ$  angle has also been tested but gave poor results for the electronic properties. Finally the pendant aromatic moieties are also close to planarity with the double bond (angle  $< 10^\circ$ ) except in the case of the mesityl **4b** where the *ortho* substituents force the phenyl ring out of plane by an angle of  $30^\circ$ .

Inspection of the molecular orbitals involved in the electronic transitions shows that the electronic delocalisation on the styryl substituents is linked to both their geometrical and electronic features. Indeed, in the case of derivatives **3c**, **4a**, **4c** and **4d** where the aromatic are electron donating groups the HOMOs are fully delocalised on the BODIPY and styryl moieties (Fig. 4). Contrariwise, in the case of **4b** the steric hindrance of the methyl groups on the mesityl moieties limit the delocalization to the double bond and in **4e** where the substituent is electron withdrawing, the orbital is mainly localized on the BODIPY core. Conversely, the lowest unoccupied MOs are localized on the BODIPY for **3c**, and **4a–d** and on the overall BODIPY-styryl part for **4e**. The next orbitals (HOMO–1 and LUMO+1) are all mainly localized on the styryl substituents.

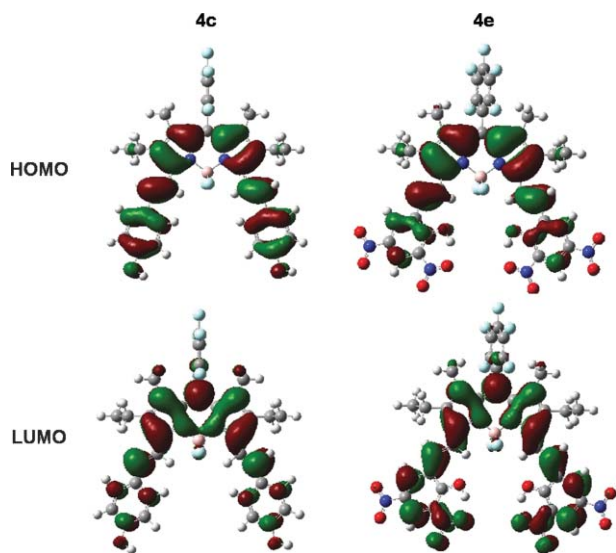


**Fig. 4** HOMO (top) and LUMO (bottom) of BODIPY **4c** (left) and **4d** (right).

Vertical absorptions of the derivatives were investigated by TDDFT method (Table 3). The PBE0 functional with 6-311+g(d,p) basis set was used because it has been shown to yield good results for organic molecules.<sup>19</sup> The first transition is found between 530 and 700 nm with an associated oscillator strength  $f$  around 0.8 (except for **4e** where it is only 0.47) which is consistent with the observed intense visible first transition for the BODIPY. The mono substituted derivative **3c** has the lowest calculated transition at 536 nm. The additional styryl in **4c** shifts this absorption toward the red by 63 nm (71 nm experimentally). The energy progression of the calculated transitions matches the experimental one except in the case of **4b**. The reason probably lies in a large difference between the geometry obtained in the minimization and the actual structure in solution. Solvent effects have been included in two cases, **4d** and **4e**, using IEFPCM model because of their highly polar nature. The calculated values are

closer to the observed ones but the nature of the transitions remains essentially unchanged.

Electronic densities differences between the first excited state and the ground state for neutral and protonated BODIPY **4d** (Fig. 5) clearly illustrate the different nature of the electronic transition. In the case of the neutral form a charge transfer occurs from the aniline rings to the BODIPY core. The final density is mainly located on the *meso* carbon. Contrariwise, the protonation of **4d** induces a reversal of the density shift as it starts from the BODIPY core and redistributes more evenly on the overall molecule. An intermediate situation is found for **4a** where the phenyl rings play a minor role in the electronic transition demonstrating the important role played by the nature of the aromatic rings on the electronic properties of this series of BODIPY.

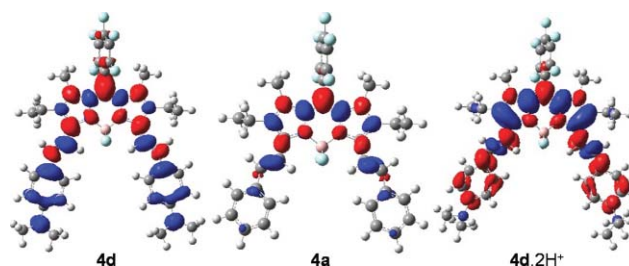


**Fig. 5** Calculated electron density changes accompanying the first electronic excitation of BODIPY **4d** (left) **4a** (middle) and **4d. 2H<sup>+</sup>** (right). The blue and red lobes signify decreases and increases respectively in electron density accompanying the electronic transition. Their areas indicate the magnitude of the electron density change.

## Conclusions

A new series of styryl appended BODIPY derivatives has been rationally designed and obtained from a new platform made of pentafluorophenyl BODIPY. BODIPY **1** can be synthesised in good overall yield and thanks to the strategic position of the fluorinated benzene, it displays good reactivity toward the Knoevenagel condensation as seen from the quasi exclusive formation of distyryl derivatives. A series of aromatic aldehydes has been used in the condensation both with electron donating groups and, for the first time, electron withdrawing ones. The derivatives obtained have clear BODIPY like spectroscopy. A charge transfer occurs in the first excited state as seen from the quantum mechanic calculations. Applicability of this BODIPY is exemplified by the important fluorescence change of BODIPY **4d** upon acidification. The BODIPY of this series should display good two photon absorption cross section. Work is in progress to introduce other substituents such as bulky or electroactive groups in order to expand the field of applicability of distyryl BODIPY to solid state fluorescence or electrochemical control of emission.<sup>20</sup>

## Experimental

### General methods

Analytical thin-layer chromatography was performed on pre-coated plates (silica gel 60, 0.25 mm, F-254). All reagents were purchased from Sigma-Aldrich Chemical Co. and were used as

received. All solvents were purchased from SDS and were used as received. Column chromatographic separations were performed using 60–230 mesh silica gel. NMR spectra were recorded on a JEOL ECS 400 MHz spectrometer. The spectra were taken with TMS as a proton standard reference (0 ppm). For  $^{13}\text{C}$  spectra, central peak of the residual solvent multiplets were used as a chemical shift reference ( $\text{CDCl}_3$ : 77.00 ppm and  $(\text{CD}_3)_2\text{CO}$ : 205.87 ppm and 30.60 ppm). Melting points (MPs) were obtained without correction with a Kofler melting point apparatus. IR spectra were measured with a Nicolet Avatar 330 FT IR. Mass spectra were measured at the CNRS Imagif platform.

**4,4-Difluoro-2,6-diethyl-1,3,5,7-dimethyl-8-perfluorophenyl-4-bora-3a,4a-diaza-s-indacene (1).** In a three necked round bottom flask charged with 100 mL of dichloromethane (DCM), were dissolved kryptopyrrole (1.0 g, 8.12 mmol, 2 eq.), perfluorobenzaldehyde (0.796 mg, 4.06 mmol, 1 eq.) and few drops of trifluoroacetic acid (TFA). When the aldehyde was consumed (monitored by TLC), add quickly the oxidation reagent chloranil (0.998 mg, 4.06 mmol, 1 eq.). After 5 min, diisopropylethylamine (3.67 g, 28.4 mmol, 7 eq.) was added. After 15 min, the boron trifluoride diethyl etherate (6.34 g, 44.6 mmol, 11 eq.) was dissolved. Purification was performed on column chromatography (silica gel,  $R_f$  0.41) using mixture of petroleum ether and dichloromethane (70/30, v/v) as eluent. The orange fluorescent fraction was collected and the removal of the solvents afforded 0.930 mg as a gold solid (mp = 204–205 °C). Yield: 94%.  $^1\text{H}$  NMR ( $\text{CDCl}_3$ )  $\delta$  1.02 (t, 6H,  $J = 7.56$  Hz), 1.51 (s, 6H), 2.34 (q, 4H,  $J = 7.63$  Hz), 2.54 (s, 6H);  $^{13}\text{C}$  NMR ( $\text{CDCl}_3$ )  $\delta$  10.18, 11.35, 12.66, 14.46, 121.21, 130.42, 134.01, 136.65, 156.21;  $^{11}\text{B}$  NMR ( $\text{CDCl}_3$ )  $\delta$  -0.27 (t,  $^1J_{\text{B}-^{19}\text{F}} = 31.99$  Hz);  $^{19}\text{F}$  NMR ( $\text{CDCl}_3$ )  $\delta$  -160.02 (m, 2F), -151.30 (t, 1F,  $^3J_{\text{F}-^{19}\text{F}} = 20.95$  Hz), -145.59 (q, 2F,  $^1J_{\text{F}-^{11}\text{B}} = 32.75$  Hz), -139.40 (dd, 2F,  $^3J_{\text{F}-^{19}\text{F}} = 23.12$  Hz;  $^3J_{\text{F}-^{19}\text{F}} = 7.22$  Hz), FTIR:  $\nu_{\text{C}=\text{C},\text{Ar}} = 1545$   $\text{cm}^{-1}$ ,  $\nu_{\text{C}=\text{N}} = 1497$   $\text{cm}^{-1}$ ; HRMS (ESI) calcd for  $\text{C}_{23}\text{H}_{22}\text{BN}_2\text{F}_7$  493.1662 found 493.1679.

**General procedure for Knoevenagel type reaction.** All reactions were carried out in a 100 mL three necked round bottom flask. Any water formed during the reaction was azeotropically removed by using Dean–Stark apparatus. In every case 10 mL of toluene as solvent was used in the reaction. After disappearance of the aldehyde (as monitored by TLC) solvent was removed under reduced pressure and crude products were purified by column chromatography.

**(4a).** A mixture of BODIPY **1** (200 mg, 0.43 mmol, 1 eq.), benzaldehyde (125 mg, 1.28 mmol, 3eq) and piperidine (72 mg, 0.85 mmol, 2 eq.) in toluene was refluxed for 24 h. The reaction mixture was cooled to room temperature and the solvent was removed under reduced pressure. The crude product was purified by column chromatography (dichloromethane/cyclohexane, 1/9, v/v). **4a** was isolated as a dark powder (36 mg, yield 13%, mp > 260 °C).  $^1\text{H}$  NMR ( $\text{CDCl}_3$ )  $\delta$  1.21 (t, 6H,  $J = 7.46$  Hz,  $\text{CH}_3-\text{CH}_2$ ), 1.57 (s, 6H,  $\text{CH}_3$ ), 2.66 (q, 4H,  $J = 7.48$  Hz,  $\text{CH}_2-\text{CH}_3$ ), 7.29–7.44 (m, 8H,  $\text{CH}_{\text{Ar}}$  and  $\text{CH}=\text{CH}$ ), 7.64 (d, 4H,  $J = 7.79$  Hz,  $\text{CH}_{\text{Ar}}$ ), 7.78 (d, 2H,  $J = 16.49$  Hz,  $\text{CH}=\text{CH}$ );  $^{13}\text{C}$  NMR ( $\text{CDCl}_3$ )  $\delta$  10.73, 14.06, 18.42, 119.01, 119.73, 127.58, 128.84, 129.06, 132.82, 134.97, 137.09, 137.34, 145.57, 152.08;  $^{11}\text{B}$  NMR ( $\text{CDCl}_3$ )  $\delta$  0.17 (t,  $J = 33.23$  Hz);  $^{19}\text{F}$  NMR ( $\text{CDCl}_3$ )  $\delta$  -159.55 (m), -150.62 (m), -138.82 (m), -138.73 (m), -138.65 (q,  $J = 32.29$  Hz); IR:

$\nu_{\text{C}=\text{C},\text{Ar}} = 1614$   $\text{cm}^{-1}$ ,  $\nu_{\text{C}=\text{N}} = 1496$   $\text{cm}^{-1}$ ; HRMS (ESI) calcd for  $\text{C}_{37}\text{H}_{30}\text{BN}_2\text{F}_7$  646.2390, found 646.2357.

**(4b).** A mixture of BODIPY **1** (227 mg, 0.48 mmol, 1eq), mesitaldehyde (214 mg, 1.45 mmol, 3 eq.) and piperidine (164 mg, 1.93 mmol, 4 eq.) was refluxed in toluene for 48 h. The reaction mixture was cooled to room temperature and the solvent was removed under reduced pressure. The crude product was purified by column chromatography (dichloromethane/petroleum ether 25/75, v/v). The first fraction afforded compound **4b** as a copper-red solid (71 mg, yield 21%, mp > 260 °C).  $^1\text{H}$  NMR ( $\text{CDCl}_3$ )  $\delta$  1.20 (t, 6H,  $J = 7.56$  Hz), 1.58 (s, 6H), 2.30 (s, 6H), 2.46 (s, 12H), 2.66 (q, 4H,  $J = 7.56$  Hz), 6.94 (broad signal s, 4H), 7.33 (d, 2H,  $J = 16.94$  Hz), 7.41 (d, 2H,  $J = 16.94$  Hz);  $^{13}\text{C}$  NMR ( $\text{CDCl}_3$ )  $\delta$  10.68, 14.14, 18.53, 21.07, 21.40, 119.20, 124.60, 132.39, 132.50, 133.52, 134.42, 135.98, 136.85, 136.98, 137.55, 152.23;  $^{11}\text{B}$  NMR ( $\text{CDCl}_3$ )  $\delta$  0.12 (t,  $J = 33.22$  Hz);  $^{19}\text{F}$  NMR ( $\text{CDCl}_3$ )  $\delta$  -159.64 (m), -150.75 (m), -139.12 (m), -138.73 (q,  $J = 32.29$  Hz); FTIR:  $\nu_{\text{C}=\text{C},\text{Ar}} = 1606$   $\text{cm}^{-1}$ ,  $\nu_{\text{C}=\text{N}} = 1496$   $\text{cm}^{-1}$ ; HRMS (ESI) calcd for  $\text{C}_{43}\text{H}_{42}\text{BN}_2\text{F}_7$  730.3329, found 730.3321.

**(3c) and (4c).** A mixture of BODIPY **1** (100 mg, 0.21 mmol, 1 eq.), *p*-hydroxybenzaldehyde (50 mg, 0.43 mmol, 2 eq.) and piperidine (0.034 mg, 0.43 mmol, 2 eq.) was refluxed in toluene for 48 h. The reaction mixture was cooled to room temperature and the solvent was removed under reduced pressure. The crude product was purified by column chromatography (ethyl acetate/petroleum ether 1/9, v/v). A blue coloured fraction containing **3c** was collected first (35 mg, yield 31%, mp > 260 °C).  $^1\text{H}$  NMR ( $\text{CDCl}_3$ )  $\delta$  1.03 (t, 3H,  $J = 7.64$  Hz), 1.18 (t, 3H,  $J = 7.64$  Hz), 1.53 (s, 3H), 1.55 (s, 3H), 2.35 (q, 2H,  $J = 7.64$  Hz), 2.58 (s, 3H), 2.62 (q, 2H,  $J = 7.64$  Hz), 6.85 (d, 2H,  $J = 8.70$  Hz), 7.22 (d, 1H,  $J = 16.94$  Hz), 7.48 (d, 2H,  $J = 8.7$  Hz), 7.57 (d, 1H,  $J = 16.94$  Hz);  $^{13}\text{C}$  NMR ( $\text{CDCl}_3$ )  $\delta$  10.63, 10.94, 14.08, 14.14, 14.54, 17.14, 18.35, 23.99, 115.78, 117.39, 117.66, 129.06, 130.00, 131.37, 134.05, 134.49, 136.47, 136.95, 151.59, 156.60, 156.82;  $^{11}\text{B}$  NMR ( $\text{CDCl}_3$ )  $\delta$  -0.019 (t,  $J = 33.22$  Hz);  $^{19}\text{F}$  NMR ( $\text{CDCl}_3$ )  $\delta$  -159.72 (m), -150.19 (m), -142.34 (m), -138.86 (q,  $J = 32.29$  Hz); FTIR:  $\nu_{\text{O-H}} = 3496$   $\text{cm}^{-1}$ ,  $\nu_{\text{C}=\text{C},\text{Ar}} = 1599$   $\text{cm}^{-1}$ ,  $\nu_{\text{C}=\text{N}} = 1498$   $\text{cm}^{-1}$ ; HRMS (ESI) calcd for  $\text{C}_{30}\text{H}_{26}\text{BN}_2\text{OF}_7$  574.2026, found 574.2030. A green fraction was then collected and afforded **4c** (50 mg, yield 37%, mp > 260 °C).  $^1\text{H}$  NMR ( $(\text{CD}_3)_2\text{CO}$ )  $\delta$  1.16 (t, 6H,  $J = 7.5$  Hz), 1.64 (s, 6H), 2.69 (q, 4H,  $J = 7.5$  Hz), 6.95 (d, 4H,  $J = 8.7$  Hz), 7.38 (d, 2H,  $J = 16.94$  Hz), 7.52 (d, 4H,  $J = 8.7$  Hz), 7.63 (d, 2H,  $J = 16.94$  Hz);  $^{13}\text{C}$  NMR ( $(\text{CD}_3)_2\text{CO}$ )  $\delta$  10.11, 13.51, 18.04, 116.07, 116.65, 128.92, 129.17, 131.17, 132.46, 134.77, 137.03, 137.33, 137.44, 151.96, 159.12;  $^{11}\text{B}$  NMR ( $(\text{CD}_3)_2\text{CO}$ )  $\delta$  0.27 (t,  $J = 34.46$  Hz);  $^{19}\text{F}$  NMR ( $(\text{CD}_3)_2\text{CO}$ )  $\delta$  -161.52 (m), -152.68 (s), -141.90 (m), -138.30 (q,  $J = 32.29$  Hz); FTIR:  $\nu_{\text{O-H}} = 3515$   $\text{cm}^{-1}$ ,  $\nu_{\text{C}=\text{C},\text{Ar}} = 1595$   $\text{cm}^{-1}$ ,  $\nu_{\text{C}=\text{N}} = 1500$   $\text{cm}^{-1}$ ; HRMS (ESI) calcd for  $\text{C}_{37}\text{H}_{30}\text{BN}_2\text{O}_2\text{F}_7$  678.2289, found 678.2271.

**(4d).** A mixture of BODIPY **1** (200 mg, 0.43 mmol, 1 eq.), *N,N*-dimethyl-4-aminobenzaldehyde (128 mg, 0.85 mmol, 2 eq.) and piperidine (109 mg, 1.28 mmol, 3 eq.) in toluene was refluxed for 48 h. The reaction mixture was cooled to room temperature and the solvent was removed under reduced pressure. The crude product was purified by column chromatography (dichloromethane/petroleum ether, 5/5, v/v). **4d** was isolated as a brown solid (118 mg, yield 38%, mp > 260 °C).  $^1\text{H}$  NMR ( $\text{CDCl}_3$ )  $\delta$  1.20 (t, 6H,  $J = 7.56$  Hz), 1.53 (s, 6H), 2.65 (q, 4H,  $J = 7.48$  Hz,

6.74 (d, 4H,  $J = 8.7$  Hz), 7.26 (d, 2H,  $J = 16.94$  Hz), 7.55 (d, 4H,  $J = 8.7$  Hz), 7.63 (d, 2H,  $J = 16.94$  Hz);  $^{13}\text{C}$  NMR ( $\text{CDCl}_3$ )  $\delta$  10.58, 14.04, 18.58, 40.34, 112.17, 115.61, 125.76, 126.14, 129.09, 134.33, 135.65, 137.25, 150.97, 151.77;  $^{11}\text{B}$  NMR ( $\text{CDCl}_3$ )  $\delta$  0.34 (t,  $J = 34.46$  Hz);  $^{19}\text{F}$  NMR ( $\text{CDCl}_3$ )  $\delta$  -160.19 (m), -151.61 (m), -139.29 (q,  $J = 32.29$  Hz), -138.64 (d,  $J = 34.46$  Hz); FTIR:  $\nu_{\text{C}=\text{C}, \text{Ar}} = 1588 \text{ cm}^{-1}$ ,  $\nu_{\text{C}=\text{N}} = 1496 \text{ cm}^{-1}$ ; HRMS (ESI) calcd for  $\text{C}_{41}\text{H}_{40}\text{BN}_4\text{F}_7$  732.3234, found 732.3265.

**(4d).** A mixture of BODIPY **1** (100 mg, 0.21 mmol, 1 eq.), 3,5-dinitrosalicylic aldehyde (100 mg, 0.47 mmol, 2.2 eq) and piperidine (69 mg, 0.85 mmol, 4eq) was refluxed in toluene during 48 h. The reaction mixture was cooled to room temperature and the solvent was removed under reduced pressure. The crude mixture was purified by column chromatography (ethyl acetate/cyclohexane, 8/2, v/v). **4e** was isolated as a green-dark solid (63 mg, yield: 36%, mp > 260 °C).  $^1\text{H}$  NMR ( $(\text{CD}_3)_2\text{CO}$ )  $\delta$  1.12 (t, 6H,  $J = 7.33$  Hz), 1.57 (s, 6H), 2.33 (q, 4H,  $J = 7.33$  Hz), 7.71 (d, 4H,  $J = 16.49$  Hz), 7.86 (d, 2H,  $J = 2.75$  Hz), 8.11 (d, 4H,  $J = 2.98$  Hz), 8.44 (d, 2H,  $J = 2.98$  Hz);  $^{13}\text{C}$  NMR ( $(\text{CD}_3)_2\text{CO}$ )  $\delta$  9.97, 13.72, 17.86, 119.78, 123.97, 128.26, 130.31, 132.43, 133.02, 133.42, 135.71, 136.07, 136.52, 137.44, 152.09, 171.21;  $^{11}\text{B}$  NMR ( $(\text{CD}_3)_2\text{CO}$ )  $\delta$  0.077 (t,  $J = 33.22$  Hz);  $^{19}\text{F}$  NMR ( $(\text{CD}_3)_2\text{CO}$ )  $\delta$  -137.92 (q,  $J = 32.29$  Hz), -142.04 (m), -149.63 (m), -158.78 (s); IR:  $\nu_{\text{C}=\text{C}, \text{Ar}} = 2853 \text{ cm}^{-1}$ ,  $\nu_{\text{O}-\text{H}} = 3513 \text{ cm}^{-1}$ .

### UV-vis and fluorescence spectroscopy

All the spectroscopic experiments were carried out in spectroscopic grade solvents from SDS and at concentrations ca. 10  $\mu\text{mol L}^{-1}$  for absorption spectra and ca. 1  $\mu\text{mol L}^{-1}$  for fluorescence spectra. UV-vis. absorption spectra were recorded on a Varian Cary 500 spectrophotometer. Fluorescence emission and excitation spectra were measured on a SPEX fluorolog-3 (Horiba-Jobin-Yvon). For emission fluorescence spectra, the excitation wavelengths were set equal to the maximum of the corresponding absorption spectra. For excitation fluorescence spectra, the emission wavelengths were set equal to the maximum of the corresponding emission spectra. For the determination of the relative fluorescence quantum yields ( $\Phi_f$ ), only dilute solutions with an absorbance below 0.1 at the excitation wavelength  $\lambda_{\text{ex}}$  were used. Sulforhodamine 101 in ethanol, ( $\Phi_f = 0.9$ ) was used as fluorescence standard for **1** and **3c** and tetraphenylazadiopyromethene boron dimethoxyde in chloroform ( $\Phi_f = 0.31$ )<sup>21</sup> was used as fluorescence standard for **4a–e**. The fluorescence decay curves were obtained with a time-correlated single-photon-counting method using a titanium/sapphire laser (82 MHz, fundamental wave: 695–1000 nm, repetition rate lowered to 4 MHz by a pulse-peaker, 1 ps pulse width) pumped by an argon ion laser. 695 nm excitation was obtained directly from the fundamental wave. A doubling crystal was used to reach 495 nm excitation.

### Molecular modelling

All calculations were performed with the Gaussian 03 program<sup>22</sup> *in vacuo* on a Nec TX7 with 32 processors Itanium 2 of the MESO centre of the ENS Cachan. Geometries have been obtained at the B3LYP/6-31g(d) level and electronic properties (molecular orbitals and vertical transitions) with PB0 functional and the 6-311g+(d,p) basis set as suggested in ref. 23. Surfaces have been

generated with the cubgen module of Gaussian and visualized with GaussView 3.0 of Gaussian Inc.

### Acknowledgements

We are indebted to Arnaud Brosseau for his assistance with the time resolved spectroscopy measurements.

### References

- 1 R. Weissleder, *Nat. Biotechnol.*, 2001, **19**, 316.
- 2 H. Hoppe and N. S. Sariciftci, *J. Mater. Res.*, 2004, **19**, 1924.
- 3 (a) T. K. Hatwar, J. P. Spindler, M. L. Ricks, R. H. Young, Y. Hamada, N. Saito, K. Mameno, R. Nishikawa, H. Takahashi and G. Rajeswaran, in *Organic Light-Emitting Materials and Devices VII*, ed. Z. H. Kafafi and P. A. Lane, SPIE, Bellingham, 2004, p. 233; (b) *Organic Light Emitting Devices*, ed. K. Müllen and U. Scherf, Wiley-VCH, Weinheim, 2006; (c) H. Langhals, O. Krotz, K. Polborn and P. Mayer, *Angew. Chem., Int. Ed.*, 2005, **44**, 2427.
- 4 *The Handbook — A Guide to Fluorescent Probes and Labeling Technologies*, Invitrogen, Molecular Probes™, <http://probes.invitrogen.com/handbook/>.
- 5 (a) A. Harriman, L. J. Mallon, S. Goebb and R. Ziessel, *Phys. Chem. Chem. Phys.*, 2007, **9**, 5199; (b) X. Zhang, Y. Xiao and X. Qian, *Org. Lett.*, 2008, **10**, 29; (c) S. Zrig, P. Remy, B. Andrioletti, E. Rose, I. Asselberghs and K. Clays, *J. Org. Chem.*, 2008, **73**, 1563.
- 6 (a) A. Coskun and E. U. Akkaya, *J. Am. Chem. Soc.*, 2005, **127**, 10464; (b) K. Yamada, Y. Nomura, D. Citterio, N. Iwasawa and K. Suzuki, *J. Am. Chem. Soc.*, 2005, **127**, 6956; (c) T. W. Hudnall and F. P. Gabbai, *Chem. Commun.*, 2008, 4596; (d) L. Zeng, E. W. Miller, A. Pralle, E. Y. Isacoff and C. J. Chang, *J. Am. Chem. Soc.*, 2006, **128**, 10; (e) M. Yuan, W. Zhou, X. Liu, M. Zhu, J. Li, X. Yin, H. Zheng, Z. Zuo, C. Ouyang, H. Liu, Y. Li and D. Zhu, *J. Org. Chem.*, 2008, **73**, 5008; (f) S. Atilgan, T. Ozdemir and E. U. Akkaya, *Org. Lett.*, 2008, **10**, 4065.
- 7 (a) H. Röhr, C. Trieffinger, K. Rurack and J. Daub, *Chem.–Eur. J.*, 2006, **12**, 689; (b) H. Sunahara, Y. Urano, H. Kojima and T. Nagano, *J. Am. Chem. Soc.*, 2007, **129**, 5597; (c) M. Tomaso, E. Deniz, R. J. Alvarado and F. M. Raymo, *J. Phys. Chem. C*, 2008, **112**, 8038.
- 8 T. Yogo, Y. Urano, Y. Ishitsuka, F. Maniwa and T. Nagano, *J. Am. Chem. Soc.*, 2005, **127**, 12162.
- 9 (a) A. Loudet, R. Bandichhor, L. Wu and K. Burgess, *Tetrahedron*, 2008, **64**, 3642; (b) A. Harriman, A. Mallon and R. Ziessel, *Chem.–Eur. J.*, 2008, **14**, 11461; (c) J. Y. Han, O. Gonzalez, A. Aguilar-Aguilar, E. Pena-Cabrera and K. Burgess, *Org. Biomol. Chem.*, 2009, **7**, 34.
- 10 (a) A. Loudet and K. Burgess, *Chem. Rev.*, 2007, **107**, 4891; (b) G. Ulrich, R. Ziessel and A. Harriman, *Angew. Chem., Int. Ed.*, 2008, **47**, 1184.
- 11 (a) L. H. Thoresen, H. J. Kim, M. B. Welch, A. Burghart and K. Burgess, *Synlett*, 1998, 1276; (b) A. Loudet, R. Bandichhor, K. Burgess, A. Palma, S. O. McDonnell, M. J. Hall and D. F. O'Shea, *Org. Lett.*, 2008, **10**, 4771; (c) W. L. Zhao and E. M. Carreira, *Chem.–Eur. J.*, 2006, **12**, 7254; (d) J. Killoran, S. O. McDonnell, J. F. Gallagher and D. F. O'Shea, *New J. Chem.*, 2008, **32**, 483.
- 12 (a) A. Coskun and E. U. Akkaya, *Tetrahedron Lett.*, 2004, **45**, 4947; (b) R. Ziessel, G. Ulrich, A. Harriman, M. A. H. Alamiry, B. Stewart and P. Retailleau, *Chem.–Eur. J.*, 2009, **15**, 1359; (c) S. Erten-Ela, M. D. Yilmaz, B. Icli, Y. Dede, S. Icli and E. U. Akkaya, *Org. Lett.*, 2008, **10**, 3299; (d) E. Deniz, G. C. Isbasar, O. A. Bozdemir, L. T. Yildirim, A. Siemarczuk and E. U. Akkaya, *Org. Lett.*, 2008, **10**, 3401; (e) W. Qin, T. Rohand, W. Dehaen, J. N. Clifford, K. Driesen, D. Beljonne, B. VanAverbeke, M. VanderAuweraer and N. Boens, *J. Phys. Chem. A*, 2007, **111**, 8588; (f) H. C. Kang and R. P. Haugland *US Pat.* 5,451,663, 1995.
- 13 (a) T. T. Vu, S. Badré, C. Dumas-Verdes, J.-J. Vachon, C. Julien, P. Audebert, E. Y. Senotrusova, E. Y. Schmidt, B. A. Trofimov, R. B. Pansu, G. Clavier and R. Méallet-Renault, *J. Phys. Chem. C*, 2009, **113**, 11844; (b) E. Y. Schmidt, B. A. Trofimov, A. b. I. Mikhaleva, N. V. Zorina, N. I. Protzuk, K. B. Petrushenko, I. A. Ushakov, M. Y. Dvorko, R. Méallet-Renault, G. Clavier, T. T. Vu, H. T. T. Tran and R. B. Pansu, *Chem.–Eur. J.*, 2009, **15**, 5823; (c) S. Badré, V. Monnier, R. Méallet-Renault, C. Dumas-Verdes, E. Y. Schmidt, A. b. I. Mikhaleva, G. Laurent, G. Levi, A. Ibanez, B. A. Trofimov and R. B. Pansu, *J. Photochem. Photobiol., A*, 2006, **183**, 238.

- 14 For a recent example on corrole see: T. Hori and A. Osuka, *Eur. J. Org. Chem.*, 2010, 2379.
- 15 (a) Y. Gabe, Y. Urano, K. Kikuchi, H. Kojima and T. Nagano, *J. Am. Chem. Soc.*, 2004, **126**, 3357; (b) S. Mula, A. K. Ray, M. Banerjee, T. Chaudhuri, K. Dasgupta and S. Chattopadhyay, *J. Org. Chem.*, 2008, **73**, 2146.
- 16 (a) K. Rurack, D. Kollmannsberger and J. Daub, *New J. Chem.*, 2001, **25**, 289; (b) S. Atilgan, I. Kutuk and T. Ozdemir, *Tetrahedron Lett.*, 2010, **51**, 892; (c) Z. Dost, S. Atilgan and E. U. Akkaya, *Tetrahedron*, 2006, **62**, 8484; (d) J.-Y. Liu, H.-S. Yeung, W. Xu, X. Li and D. K. P. Ng, *Org. Lett.*, 2008, **10**, 5421.
- 17 J. Catalán, *J. Phys. Chem. B*, 2009, **113**, 5951.
- 18 J. Catalán and H. Hopf, *Eur. J. Org. Chem.*, 2004, 4694.
- 19 (a) V. Barone and A. Polimeno, *Chem. Soc. Rev.*, 2007, **36**, 1724; (b) D. Jacquemin, E. A. Perpète, I. Ciofini and C. Adamo, *Acc. Chem. Res.*, 2009, **42**, 326.
- 20 F. Miomandre, R. Meallet-Renault, J. J. Vachon, R. B. Pansu and P. Audebert, *Chem. Commun.*, 2008, 1913.
- 21 A. Palma, M. Tasiór, D. O. Frimannsson, T. T. Vu, R. Méallet-Renault and D. F. O'Shea, *Org. Lett.*, 2009, **11**, 3638.
- 22 M. J. Frisch, G. W. Trucks, H. B. Schlegel, G. E. Scuseria, M. A. Robb, J. R. Cheeseman, J. A. Montgomery, Jr., T. Vreven, K. N. Kudin, J. C. Burant, J. M. Millam, S. S. Iyengar, J. Tomasi, V. Barone, B. Mennucci, M. Cossi, G. Scalmani, N. Rega, G. A. Petersson, H. Nakatsuji, M. Hada, M. Ehara, K. Toyota, R. Fukuda, J. Hasegawa, M. Ishida, T. Nakajima, Y. Honda, O. Kitao, H. Nakai, M. Klene, X. Li, J. E. Knox, H. P. Hratchian, J. B. Cross, V. Bakken, C. Adamo, J. Jaramillo, R. Gomperts, R. E. Stratmann, O. Yazyev, A. J. Austin, R. Cammi, C. Pomelli, J. Ochterski, P. Y. Ayala, K. Morokuma, G. A. Voth, P. Salvador, J. J. Dannenberg, V. G. Zakrzewski, S. Dapprich, A. D. Daniels, M. C. Strain, O. Farkas, D. K. Malick, A. D. Rabuck, K. Raghavachari, J. B. Foresman, J. V. Ortiz, Q. Cui, A. G. Baboul, S. Clifford, J. Cioslowski, B. B. Stefanov, G. Liu, A. Liashenko, P. Piskorz, I. Komaromi, R. L. Martin, D. J. Fox, T. Keith, M. A. Al-Laham, C. Y. Peng, A. Nanayakkara, M. Challacombe, P. M. W. Gill, B. G. Johnson, W. Chen, M. W. Wong, C. Gonzalez and J. A. Pople, *GAUSSIAN 03 (Revision C.02)*, Gaussian, Inc., Wallingford, CT, 2004.
- 23 (a) V. Barone and A. Polimeno, *Chem. Soc. Rev.*, 2007, **36**, 1724; (b) D. Jacquemin, E. A. Perpète, I. Ciofini and C. Adamo, *Acc. Chem. Res.*, 2009, **42**, 326.